MID-AMERICA TRANSPORTATION CENTER

Report # MATC-UI: 372

Final Report
25-1121-0001-372

Improving Freight Fire Safety: Experiment Testing and Computer Modeling to Further Development of Mist-Controlling Additives for Fire Mitigation

Albert Ratner, Ph.D.
Assistant Professor
Department of Mechanical and Industrial Engineering
University of Iowa

Yan Zhang, Ph.D. Candidate
Graduate Research Assistant

The University of Iowa

2012

A Cooperative Research Project sponsored by the U.S. Department of Transportation Research and Innovative Technology Administration

Improving Freight Fire Safety: Experiment Testing and Computer Modeling to Further Development of Mist-Controlling Additives for Fire Mitigation

Albert Ratner, Ph.D.
Assistant Professor
Department of Mechanical and Industrial Engineering
University of Iowa

Yan Zhang, Ph.D. Candidate
Graduate Research Assistant
Department of Mechanical and Industrial Engineering
University of Iowa

A Report on Research Sponsored by

Mid-America Transportation Center

University of Nebraska-Lincoln

August 2012

Technical Report Documentation Page

1. Report No. 25-1121-0001-372	2. Government Accession No.	3. Recipient's Catalog No.
4. Title and Subtitle Improving Freight Fire Safety: Experiment Testing and Computer Modeling to Further Development of Mist-Controlling Additives for Fire Mitigation		5. Report Date August 2012 6. Performing Organization Code
7. Author(s) Albert Ratner and Yan Zhang		8. Performing Organization Report No. 25-1121-0001-372
9. Performing Organization Name and Address Mid-America Transportation Center 2200 Vine St. PO Box 830851 Lincoln, NE 68583-0851		10. Work Unit No. (TRAIS) 11. Contract or Grant No.
12. Sponsoring Agency Name and Address Research and Innovative Technology Administration University Transportation Centers Program Department of Transportation 1200 New Jersey Avenue, SE Washington, DC 20590		13. Type of Report and Period Covered Final Report, Jan. 2010 – Dec. 2010 14. Sponsoring Agency Code MATC TRB RiP No. 24482
15. Supplementary Notes		

16. Abstract

With the purpose to minimize or prevent crash-induced fires in road and rail transportation, the current interest in bio-derived and blended transportation fuels is increasing. Based on two years of preliminary testing and analysis, it appears to be clear that polymeric additives may be added to diesel fuel to mitigate the formation of fine mists while allow regular flow through the fuel system. In this work, computer modeling was adapted as a fast and cost-effective methodology to identify the target range where polymeric additives could impact the shear-thickening effect on fuels. The Volume of Fraction (VOF) method was used within the commercial software Fluent to compute droplet behavior. Two new computational models, the combined SCA-DCA model with Jiang's correlation and the SCA-DCA model with exponential fitting, were proposed and imposed as the boundary conditions, showing a best-fit behavior with the experiment results.

17. Key Words Fire-safety, fuel droplets, fuel mist	18. Distribution Statement		
19. Security Classif. (of this report) Unclassified	20. Security Classif. (of this page) Unclassified	21. No. of Pages 22	22. Price

Table of Contents

List of Figures

List of Tables

List of Abbreviations and Nomenclature

u = Impact speed of the drop
D = Initial drop diameter
d = Drop spread diameter at a given time
t = Time measured from the instant of impact
μ = viscosity of the liquid
σ = Liquid-air surface tension
θ_s = Static contact angle
θ_D = Dynamic contact angle
V = Spreading velocity
SCA = static contact angle
DCA = dynamic contact angle
VOF = volume of fluid method

Acknowledgements

The authors acknowledge Neeraj Kumar Mishra for his experimental data. The authors thank the USDOT-RITA for their support through a Mid-America Transportation Center (MATC) grant to the University of Nebraska–Lincoln.

Disclaimer

The contents of this report reflect the views of the authors, who are responsible for the facts and the accuracy of the information presented herein. This document is disseminated under the sponsorship of the Department of Transportation University Transportation Centers Program, in the interest of information exchange. The U.S. Government assumes no liability for the contents or use thereof.

Abstract

With the purpose to minimize or prevent crash-induced fires in road and rail transportation, the current interest in bio-derived and blended transportation fuels is increasing. Based on two years of preliminary testing and analysis, it appears to be clear that polymeric additives may be added to diesel fuel to mitigate the formation of fine mists while allow regular flow through the fuel system. In this work, computer modeling was adapted as a fast and cost-effective methodology to identify the target range where polymeric additives could impact the shear-thickening effect on fuels. The Volume of Fraction (VOF) method was used within the commercial software Fluent to compute droplet behavior. Two new computational models, the combined SCA-DCA model with Jiang's correlation and the SCA-DCA model with exponential fitting, were proposed and imposed as the boundary conditions, showing a best-fit behavior with the experiment results.

Chapter 1 Introduction

The addition of long chained polymers to diesel has been proposed as a method to prevent the break-up of diesel fuel into a fine mist in transportation related accidents so as to prevent crash-induced fires (1). It was noticed that diesel fuels with long-strand polymer additives induce a non-Newtonian shear-thickening behavior (2). To identify the target range where polymer additives impart a shear-thickening effect on fuels without affecting the normal functioning of the fuel system, the variable shear stress of these fuels needs to be studied. The impact of drops of diesel on a solid surface, as a basic component of various natural and industrial processes, is a neat model to investigate the variable viscosity and shear stress of the liquids. The dynamics of fuel drop spreading on a flat smooth surface is studied in this work as a starting point for the reference of non-Newtonian behavior investigation in the future.

Droplets impacting on a solid surface have three different interaction modes: bouncing, spreading, and splashing, which occur due to the interactions of initial drop speed, pressure, surface roughness, drop viscosity and surface tension. Particularly, the impact of a diesel or methanol drop on a flat smooth surface is experimentally studied using high-speed cameras and serves as a baseline for this work (3). After a fuel drop contacts the solid surface, the liquid normally starts spreading out smoothly (4). Such smooth motion of liquid results in an expanding liquid disk called a lamella. Basically, there are four stages that occur when a fuel drop impacts a solid surface: the kinematic phase, the spreading phase, the relaxation phase and the wetting/equilibrium phase (5). First, spreading is greatly influenced by the initial kinetic energy of the drop, where the liquid is compressed and a shock wave is formed. As the impact progresses, the kinetic energy of the drop is dissipated by a viscous process in the lamella and is transformed into additional surface energy. As the drop achieves its maximum diameter, the

liquid in the lamella may rebound, and in extreme cases drops may bounce off after the surface altogether. Such oscillations are influenced by surface roughness (6) and wettability of the system (solid-liquid-gas) (7). If the undulations along the rim develop further, corona break up can occur resulting in outer edge splashing (8). Figure 1.1 (5) shows the four different stages of drop impact on a solid surface in terms of spread factor, which is the ratio of spreading diameter over initial diameter ($\beta = d/D$). Of particular interest here, when a diesel or methanol drop reaches its maximum diameter, is the case when the lamella expansion stops and the drop is stabilized (as the dotted line illustrates in fig. 1.1). This limited regime of two spreading phases is also reflected in the analysis of the evolution of the contact angles, which is discussed in great detail later in this report.

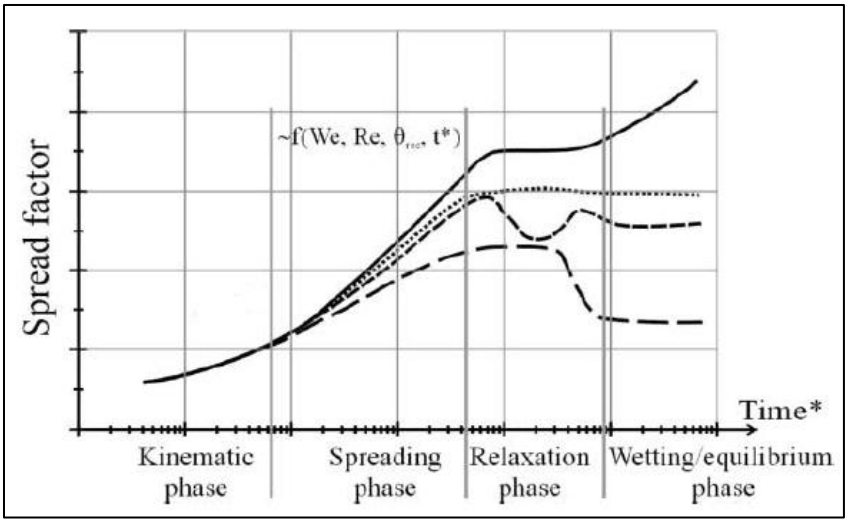

Figure 1.1 Schematic representation of the spread factor with time

NOTE: The different lines correspond to an arbitrary choice of possible spreading histories, depending on the parameters of the impact (4).

In recent years, computational fluid dynamics (CFD) has been used to predict and explain the complex hydrodynamics of drop impacting and spreading on a solid surface (9-14). Both

theoretical and empirical models have been developed for numerical analysis of these phenomena. In particular, boundary conditions at the moving contact line of the spreading drop need to be specified in terms of contact angles. Typically, there are two kinds of contact angles that are of great concern: the static contact angle θ_e (SCA) and the dynamic contact angle θ_d(DCA). According to Young's equation,

$$\sigma cos\theta_e = \sigma_{sv} - \sigma_{sl}, \tag{1.1}$$

the static contact angle is ideally a property of the system, related to the surface tension of the solid/vapor σ_{sv} and solid/liquid σ_{sl} interfaces (11). On the contrary, the dynamic contact angle θ_d is not a material property but depends (at best) on the capillary number, $Ca = \upsilon\mu/\sigma$, and (at worst) has to be experimentally measured for each drop condition. However, the exact expression of a dynamic contact angle θ_d in terms of *Ca* is still unknown. The understanding of variable θ_d has been investigated both theoretically and empirically (9, 11, and 14). In considering how and what numerical analysis to perform, the precision of these models, the physical properties, and behavior information required are all important as they impact not only the accuracy, but also the computational cost.

In this research, numerical analysis of diesel drops spreading on a flat glass surface in 3D was performed with the experimental data taken from high-speed imaging as the baseline. The volume of fluid (VOF) method (15), which is suited for large topology changes and has a low computational cost, is implemented here with the commercial software Fluent 12.0.16. To significant improve accuracy versus the SCA model and reduce the behavior information

required as compared to the full DCA model, two combined SCA-DCA models are proposed here in terms of a theoretical and an empirical correlation.

Chapter 2 Contact Angle Models

2.1 Two regimes of θ_d

The trends of dynamic contact angle θ_d were investigated for both diesel and methanol drops based on the experimental pictures. Table 2.1 shows the properties of the liquids studied. The fuel drops' initial diameters were roughly the same (diesel ~ 2.16 mm; methanol ~ 2.63 mm) whereas the impact velocity ranges from 0.7 to 3 m/s as given in table 2.2.

Table 2.1 Properties of the liquid

Liquid	σ (mN/m)	μ (mPa s)	$\rho\left(\frac{\text{kg}}{\text{m}^3}\right)$
Diesel	28.0	3.6	880
Methanol	22.7	0.6	792

Table 2.2 List of experiments

Experiment	Liquid	Impact velocity (m/s)	We	Ca
1	Diesel	1.60	177	0.205
2	Diesel	1.21	100	0.155
3	Diesel	0.76	40	0.099
4	Methanol	2.40	531	0.062
5	Methanol	2.75	691	0.071
6	Methanol	3.05	848	0.495

The values of the dynamic contact angles during fuel drop spreading have been experimentally measured and scaled in terms of the non-dimensional time *tu/D*. As reported in

Yan and Ratner's paper (16), two apparent regimes are visible in the trends of θ_d for diesel drop shown in fig. 2.1(a). The first regime corresponding to the kinetic phase of drop spreading is dominated by kinetic energy, while in the second one, viscosity and surface tension energy are the main effects, slowing the drop spreading and finally bringing the droplet to an equilibrium state. The trends of contact angles are also clear in the resulting plot: the contact angles are approximately constant in regime I, and there is a significant decrease in the contact angle during the regime II. The same situation occurs to methanol drop as presented in figure 2.1(b).

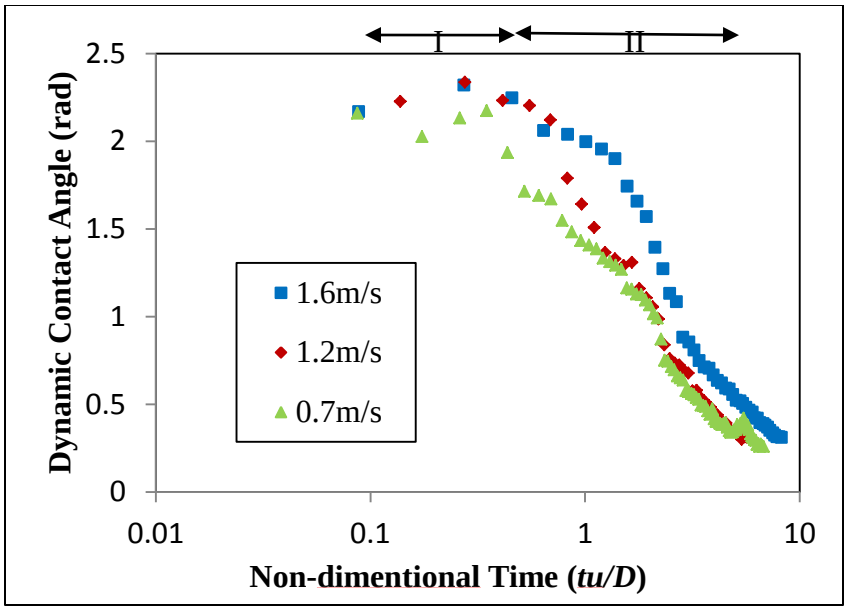

(a)

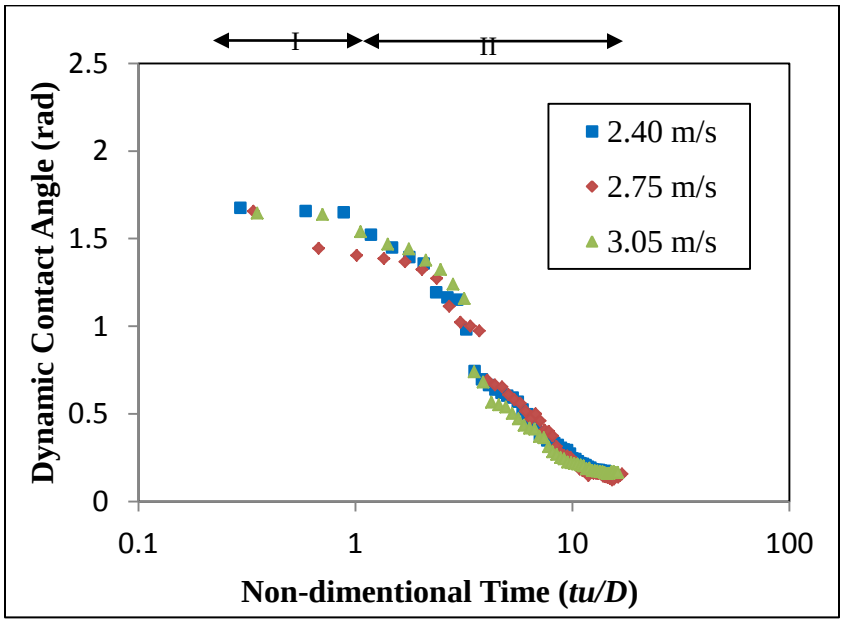

(b)

Figure 2.1 Experimental values of dynamic contact angles for fuel drops impacting at three different impact speeds

NOTE: a) diesel drop (16); b) methanol drop

All three cases exhibit two distinct regimes for each liquid, as mentioned earlier. However, the transition time (t^*) marking the change from one regime to the other (based on maximum contact angle) shows dependence on the impact speed. Particularly, for diesel droplets, the transition from regime I to regime II occurs earlier for low impact speeds, with figure 2.2 showing a nearly linearly relationship between t^* and the initial kinetic energy. Here, the initial kinetic energy is defined as $\frac{1}{2}u^2$, where u is the initial velocity. As is evident in figure 2.3, by removing regime I and starting all three plots at t^*, the behavior in regime II closely coincides for both liquids. From this, the implication is that regime II behavior has no dependence on the initial kinetic energy. Such two distinguished regimes indicate that two different numerical models should be applied for the contact angles as the boundary conditions. A static contact angle (SCA) model is identified to be sufficient to simulate regime I (16) but shows poor prediction in regime II. In that case, a more precise model is required for regime II as discussed below.

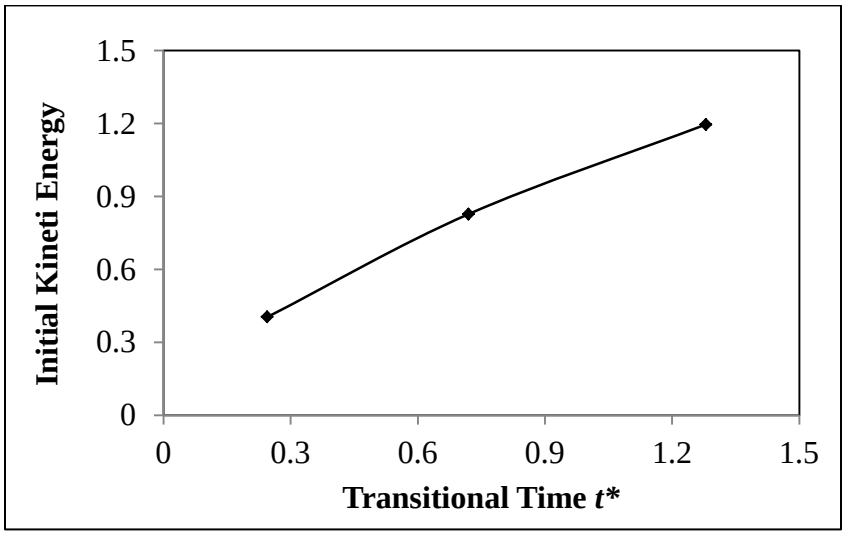

Figure 2.2 Relation of the initial kinetic energy and transitional time for diesel droplets

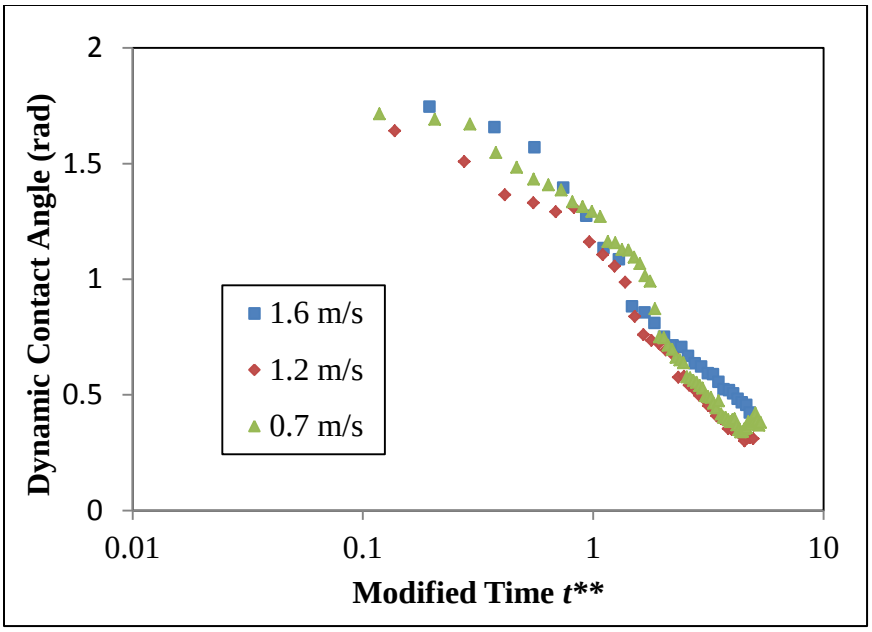

(a)

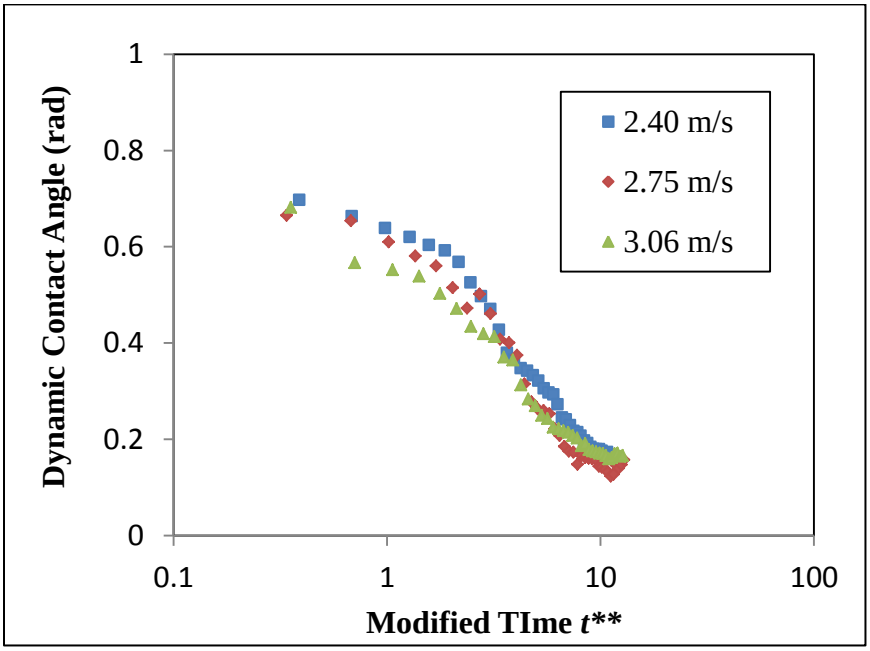

(b)

Figure 2.3 Coincided regime II of experimental values of dynamic contact angles for diesel drops (a) and methanol drop (b) (16)

2.2 Jiang's Correlation

Based on the most widespread working relation describing the contact angle for small capillary number *Ca*, the so-called Hoffman-Voinov-Tanner law (17), Jiang *et al*. (18) deduced an explicit correlation for the function $\theta_d(Ca)$ $(4 \times 10^{-5} < Ca < 36)$,

$$\frac{\cos\theta_e - \cos\theta_d}{\sin\theta_e + 1} = \tanh 4.96 Ca^{0.702} \tag{2.1}$$

The intent here is to avoid the detailed data that is required for full DCA models. The *Ca* number and SCA are functions only of the properties of the fluid and solid surface being investigated, and this allows for them to be known and the model computed without extensive experimental testing. By using the *Ca* number as the key parameter, Jiang's model allows the computation to use the spreading velocity computed in the previous time-step as the input for the *Ca* number calculation in the current time-step, which is then used to compute the contact angle. Jiang's model was the simplest model that appeared to be sufficient for this study.

The velocity used for the *Ca* number calculation is based on the speed of displacement at the interface. Since the spreading diameters can be obtained in each time step using the Fluent software, this velocity can be derived by calculating the difference in spread diameters at each time step and dividing by the time step size.

2.3 Experimental exponential correlation

Regime II shows the exact same trend for both diesel and methanol drops with various impact velocities. From this, two similar exponential trend lines can be deduced to accurately describe the measured behavior.

For a diesel drop:

$$\theta_d = \exp(4.72 - 0.51t + 0.03t^2) \tag{2.3}$$

For a methanol drop:

$$\theta_d = \exp(3.78 - 0.19t + 0.0038t^2) \tag{2.4}$$

Basically, the two exponential equations have similar format in terms of various factors. This is because diesel and methanol have similar surface tension which dominates the second regime. Again, by implementing the above equations, the detailed data that is required for full DCA models can be avoided. Since contact angles in the exponential equations only depend on time *t*, less information is required to calculate the values, resulting in less computational cost than with Jiang's correlation.

Chapter 3 Computational Method

3.1 Computational method

Two different phases are defined in the VOF method, where gas is normally defied as the primary phase whereas liquid is the secondary phase. Each control volume only contains one phase (or the interface between phases). The mass and momentum conservation equation for each phase appears as:

$$\frac{\partial(\rho u_i)}{\partial x_j} = 0 \tag{3.1}$$

$$\frac{\partial(\rho u_i)}{\partial t} + \frac{\partial}{\partial x_j}(\rho u_i u_j) = -\frac{\partial p}{\partial x_i} + \frac{\partial}{\partial x_j}\mu\left(\frac{\partial u_i}{\partial x_j} + \frac{\partial u_j}{\partial x_i}\right) + \rho g_i + F_i, \tag{3.2}$$

where u is the velocity, p is the pressure, and F is the surface tension force per unit volume. The mixture property, ϕ, is calculated as

$$\phi = \frac{\sum \varepsilon_k \rho_k \phi_k}{\sum \varepsilon_k \rho_k} \tag{3.3}$$

where ρ_k is the density of kth fluid, and ε_k is the volume fraction of the kth fluid:

$$\varepsilon_k(cell) = \frac{\iiint_{cell} \varepsilon_k(x,y,z)dxdydz}{\iiint_{cell} dxdydz} \tag{3.4}$$

When in a specified control volume, three conditions are possible:

- $\varepsilon_k = 0$: if the cell is empty (of the kth fluid)
- $\varepsilon_k = 1$: if the cell is full (of the kth fluid)
- $0 < \varepsilon_k < 1$: if the cell contains the interface between the fluids

Tracking of interface(s) between phases is accomplished by solution of a volume fraction continuity equation for each phase:

$$\frac{\partial \varepsilon_k}{\partial t} + u_j \frac{\partial \varepsilon_k}{\partial x_i} = S_{\varepsilon_k} \tag{3.5}$$

Mass transfer between phases can be modeled by using a user-defined subroutine to specify a nonzero value for S_{ε_k}. In the present work, since the mass transfer between two phases is zero, S_{ε_k} is set to be zero. The volume fraction for the primary phase is obtained directly from the following equation:

$$\sum_k \varepsilon_k = 1 \tag{3.6}$$

3.2 Numerical grid

Even though 3D simulations of normal drop spreading on a flat surface could be considered as axisymmetric with the exception of small capillary waves, a whole-drop domain is applied here rather than using quarter-drop domain (axisymmetric). This is because in the quarter drop domain the restriction on drop intrinsic instability induces an over-predicted spreading velocity (16). In this work, the solution domain represents a 12 × 12 × 5 mm large block in *x*-*y*-*z* Cartesian coordinate system, according to the maximum spreading diameter for the diesel droplet (~8 mm). As shown in figure 3.1, a structured grid with refinement close to the wall is used for discretizing the domain. It has been approved by Bussmann *et al*. (9) that a grid size with 10 cpr (cells per radius) is enough to capture the dynamics of drop spreading. In that case, the minimum

thickness of the cell employed is around 20 microns, while the radius for the diesel drop is around 1 mm and the spreading lamella is in the order of 0.1 mm.

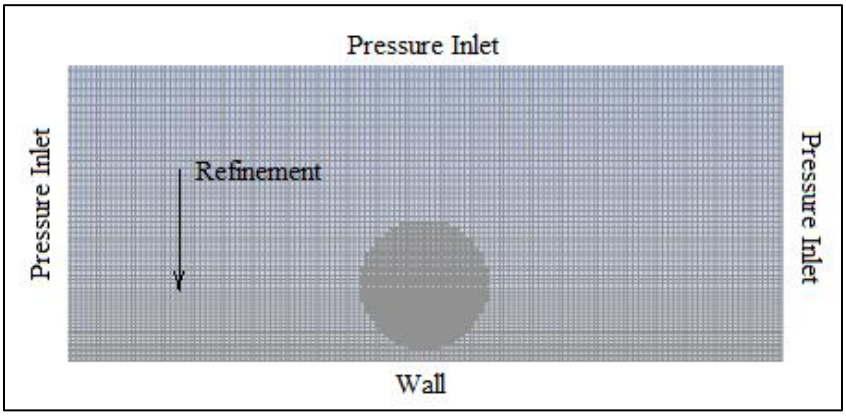

Figure 3.1 Solution domain and boundary conditions

3.3 Numerical solution and boundary conditions

A whole drop is patched in the solution domain with exactly the same diameter and initial velocity as the experimental picture shows (fig. 3.1). The bottom of the solution domain is defined as the wall while other surfaces are set as pressure-inlets. No-slip boundary condition is specified at the wall where all the components of velocity are set to be zero. Three different models of contact angles are tested in this work: the SCA model, the SCA-DCA model with Jiang's correlation, and the SCA-DCA model with exponential correlation. More details will be explained in the discussion. The QUICK scheme is implemented for the mass and momentum equations and the first-order implicit method is used to discretize the time derivatives. In the momentum equation, pressure and velocity is coupled by the pressure implicit with splitting of operator (PISO) scheme. The applied time step is varying from 0.75 to 2.48 μs corresponding to the time interval between successive frames of experimental images taken at different camera speeds.

Chapter 4 Numerical Results and Discussion

4.1 Numerical results for drop shapes

A criterion used in this work to compare the experimental and numerical results is a qualitative comparison of the spread diameter at each time step after drop impacting on the surface.

Figure 4.1 shows the comparison of experimental and numerical spreading factors for the diesel droplet with initial velocity u = 1.6 m/s. Three different models of contact angles are tested in this work: the SCA model, the SCA-DCA model with Jiang's correlation, and the SCA-DCA model with exponential correlation. Presently, the pure SCA model, for diesel drops with u = 1.6 m/s, is sufficient to accurately predict regime I, but provides poor prediction in regime II (16).

Based on the above limitation, the new models for specifying the dynamic contact angles is necessary for greater accuracy in describing the shape of the drop spread upon impact. The drop spreading is nearly identical for both the SCA model simulation and the experimental results before a critical dimensionless time tu/D (typically, for the diesel droplet with 1.6 m/s initial velocity, the critical tu/D = 0.8). Therefore, the SCA model is sufficient to accurately predict in this regime. For the regime beyond this critical time, where the drop spreading is strongly dependent of contact angles, a DCA model associated with Jiang's equation or exponential fitting is implemented with a user-defined function (UDF) to specify the contact angles for a more accurate prediction of the spread diameters.

As shown in figure 4.1, at the end of the diesel droplet spreading process, the error in spread factor for the pure SCA model is around 16.5% whereas SCA-DCA (Jiang) model is about 9%. Moreover, by using SCA-DCA (exponential) model, a significant improvement for

the drop shape's accuracy is visible: the error in spread factor at the end of drop spreading process is only about 2%.

With such a strong accuracy and much less computational cost, the SCA-DCA model with exponential equation is also tested for diesel drops with u = 1.2 m/s and u = 0.7 m/s. The numerical results are compared with the pure SCA model and experimental data (fig. 4.2). It is clear that this SCA-DCA model is sufficient to predict the drop shapes during the whole spreading process.

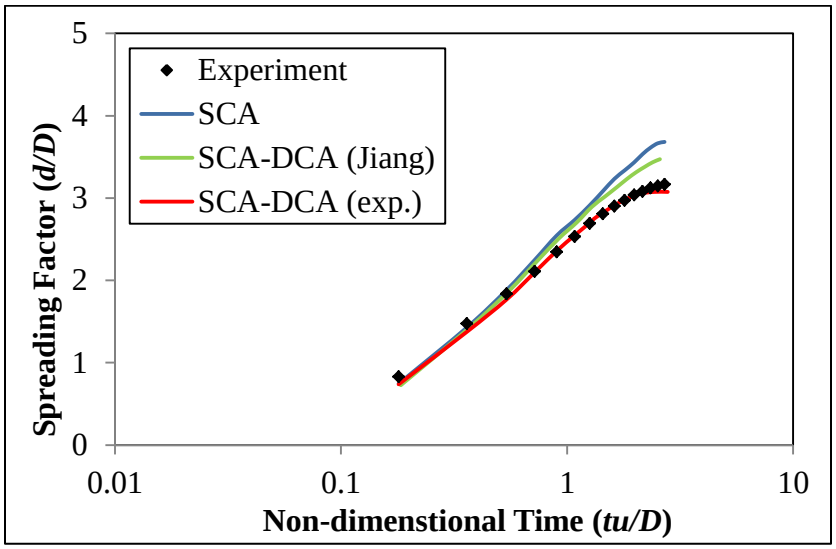

Figure 4.1 Comparison of the experimental and numerical spread factors of a diesel drop with u = 1.6 m/s

NOTE: Dotted line=experimental data; blue line=pure SCA model; green line=the SCA-DCA model with Jiang's correlation (16); red line-the SCA-DCA model with exponential correlation.

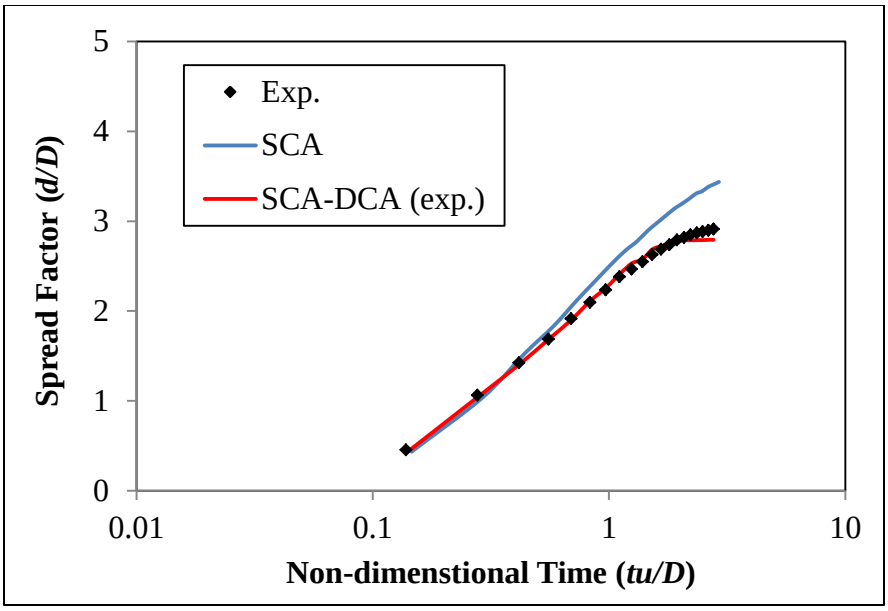

(a)

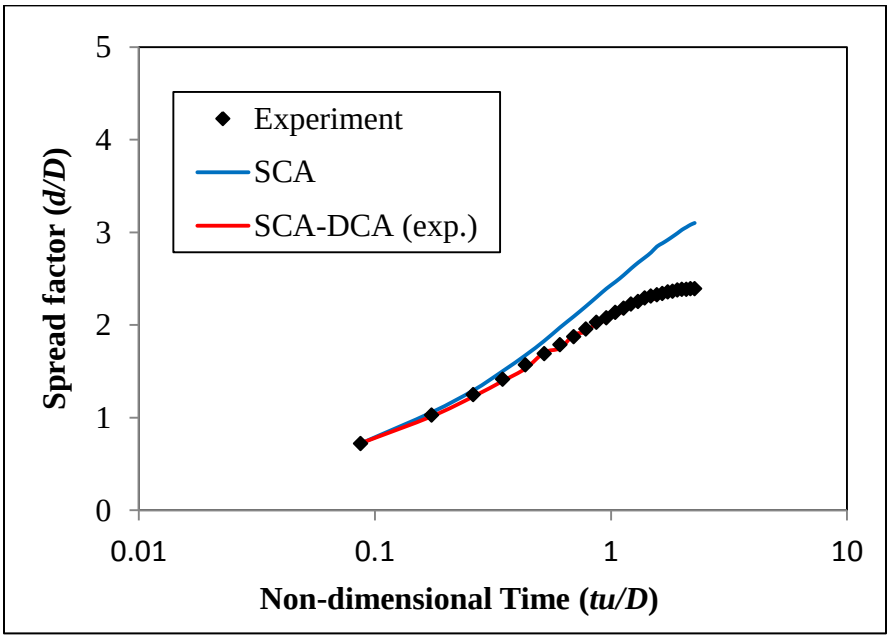

(b)

Figure 4.2 Comparison of the experimental and numerical spread factors of a diesel drop with u = 1.2 m/s (a) and u = 1.2 m/s (b)

NOTE: Dotted line=experimental data; blue line=pure SCA model; red line=the SCA-DCA model with exponential correlation.

4.2 Numerical results for the strain rate

Based on the best-fit drop shapes, the evolution of strain rate for the diesel drop can be investigated. Figure 4.3 shows a case in which the impact velocity was 1.6 m/s. It is visible that as time evolves the maximum strain rate decreases from 9×10^4 to $1.6 \times 10^4\ s^{-1}$. Namely, the maximum shear stress roughly ranges from 324 to 57 Pa during the dimensionless time between 0.18 and 1.74.

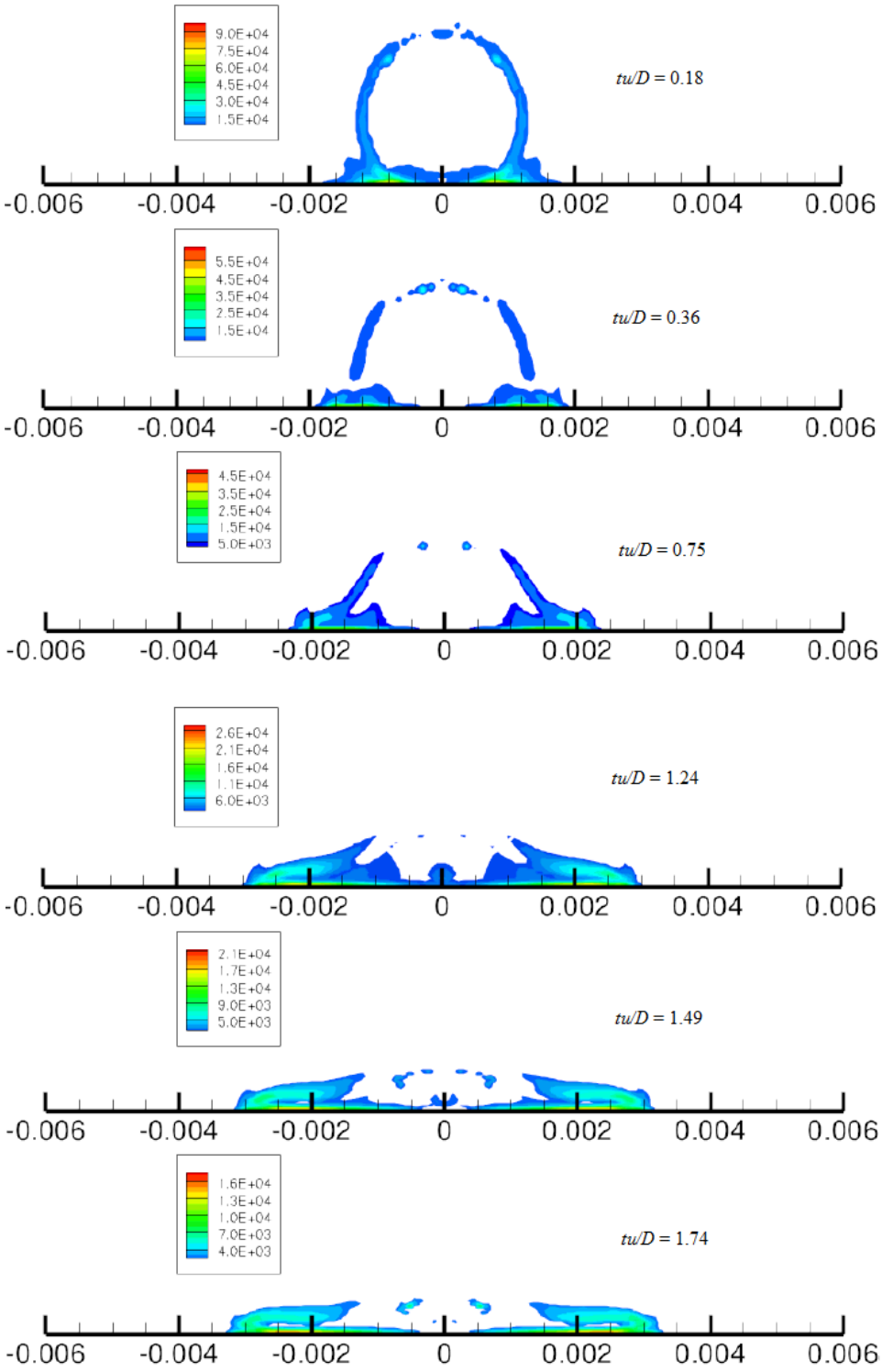

Figure 4.3 Evolution of strain rate for the diesel drop with u = 1.6 m/s

Chapter 5 Conclusion

The impact of fuel drops on a flat solid surface was numerically studied based on preliminary experimental data. The Volume of Fraction (VOF) method was employed with the Fluent commercial software package to compute the droplet behavior from impact through the spreading process. The evolution of contact angles for both diesel and methanol drops was investigated as the specified boundary condition for the numerical simulations. Two distinct regimes were observed in the evolution of the contact angles, corresponding to the kinetic phase and the spreading phase of the droplet impact process. Based on these observations and a lack of an existing model of suitable accuracy, a new combined SCA-DCA model was proposed (utilizing different coefficients for Methanol and Diesel). As the SCA model is sufficient to predict the droplets behavior in the first regime, it is employed there, while an exponential fit is employed to accurately capture the behavior during the second phase of the spreading process. The resulting model significantly improves the accuracy achievable in relation to the experimental data.

As the droplets shapes could now be accurately predicted, the strain rate evolution was also assessable in the range of interest for diesel drop spreading. Future work should modify the viscosity of the droplets to investigate the dynamics of non-Newtonian fuels.

References

1. Ratner, A. 2009. "Mitigating Crash Fires with Fuel Additives." *UTC Spotlight Newsletter*. February.

2. Ameri David, R. L., Ming-Hsin Wei, David Liu, Brett F. Bathel, Jan P. Plog, Albert Ratner, and Julia A. Kornfield. 2009. Effects of Pairwise, Self-Associating Functional Side Groups on Polymer Solubility, Solution Viscosity, and Mist Control. *Macromolecule* 42 (4):1381-1391.

3. Mishra, N.K. 2009. Effect of Chamber Pressure on Liquid Drop Impacts on a Stationary Smooth and Dry Surface. M.S. thesis, Iowa Univ.

4. Rein, M. 1993. Phenomena of liquid drop impact on solid and liquid surfaces. *Fluid Dynamics Research* 12:61-93.

5. Rioboo, R., M. Marengo, and C. Tropea. 2002. Time evolution of liquid drop impact onto solid, dry surface. *Experiments in Fluids* 33:112-124.

6. Engel, O. 1955. A water drop collision with solid surfaces. *PJ Res Nat Bur Stand* 54:281-298.

7. Woerhington, A. 1877a. On the forms assumed by drops of liquids falling vertically on a horizontal plate. *Proc R Soc London* 25:261-271.

8. Xu, L., W. Zhang, and S. R. Nagel. 2005. Drop splashing on a dry smooth surface. *Physical Review Letters* 94 (18):184505 1-4.

9. Bussmann, M., J. Mostaghimi, and S. Chandra, 1999. On a three-dimensional volume tracking model of droplet impact. *Physics of Fluids* 11:1406-1417.

10. Bussmann, M., S. Chandra, and J. Mostaghimi. 2000. Modeling the splash of a droplet impacting a solid surface. *Physics of Fluids* 12:3121-3132.

11. Sikalo, S., H. Wilhelm, I. Roisman, S. Jakirli, and C. Tropea. 2005. Dynamics contact angle of spreading droplets: Experiments and simulations. *Physics of Fluids* 17 (6):062013 1-13.

12. Gunjal, P., V. Ranade, and R. Chaudhari. 2005. Dynamics of drop impact on solid surface: experiments and VOF simulations. *AIChE Journal* 51:59-78.

13. Lunkad, S., V. Buwa, and K. Nigam. 2007. Numerical simulations of drop impact and spreading on horizontal and inclined surfaces. *Chemical Engineering Science* 62:7214-7224.

14. Pasandideh-Fard, M., Y, Qiao, S. Chandra, and J. Mostaghimi. 1996. Capillary effects during droplet impact on a solid surface. *Physics of Fluids* 8:650-659.

15. Hirt, C., and B. Nichols. 1981. Volume of fluid /VOF/ method for the dynamics of free boundaries. *Journal of Computational Physics* 39:201-225.

16. Zhang, Y., and A. Ratner. 2010. Fuel drop spreading on a flat smooth surface: numerical simulations with a VOF method. *ASME 2010 International Mechanical Engineering Congress & Exposition.* Vancouver, British Columbia, Canada: ASME.

17. Hoffman, R. 1975. A study of the advancing interface. I. Interface shape in liquid-gas systems. *J. Colloid Interface Science* 50:228-241.

18. Jiang, T., S. Oh, and J. Slattery. 1979. Correlation for dynamic contact angle. *Journal of Colloid and Interface Science* 69:74-77.